BioEnergy Research (2026) 19:116
https://doi.org/10.1007/s12155-026-11049-5

RESEARCH

Blending PCI Coal and Biochar as Sustainable Alternative for Blast Furnace Fuels

Elias R. D. Padilla[1] · Daniela A. Mortari[2] · Carlos M. R. Luna[3] · Cristiane I. de Campos[3] · Carmen Barriocanal[4] · Rafaela S. Resende[5] · Fabio M. Yamaji[5]

Received: 5 May 2026 / Accepted: 20 August 2026

Abstract

The aim of this study was to investigate the feasibility of using biochar or its blends with pulverized coal injection (PCI) coal as a potential blast furnace (BF) fuel. A comparison was conducted between the properties of biochar obtained from the pyrolysis of coconut shell and PCI coal. Coconut shells were pyrolyzed at different temperatures (between 200 °C and 450 °C) to produce biochar. The physicochemical characteristics and combustion indices of the materials were evaluated. Combustion rate was also studied using thermogravimetric analysis (TGA) to determine the effect of biochar addition on the PCI coal. Based on the combustion indices (Tmax, DTGmax, biochar yield at Tmax, and residue at 900 °C) and the three-stage thermal decomposition behavior observed in the TG/DTG analysis, it was found that biochars produced at low pyrolysis temperatures exhibited suitable characteristics for use as an auxiliary fuel in the BF. It was also observed that biochar had a higher alkalinity index (AI = 32.40) compared to the reference PCI coals (AI = 3.08 and 2.06). The results suggested that the addition of biochar coal increases the combustion rate of the resulting blends. Blends containing 10%, 30%, and 50% biochar (C200) were evaluated, corresponding to biochar/PCI coal ratios of 10/90, 30/70, and 50/50, respectively. Although biochar cannot be used as a complete replacement of PCI coal in a BF, the blend containing 30% biochar and 70% PCI coal (30% C200) showed promising performance without significantly altering fuel characteristics, demonstrating the potential of an integrated approach combining physicochemical characterization, combustion behavior, and blend performance for PCI applications.

✉ Rafaela S. Resende
rresende@estudante.ufscar.br

[1] Department of Production Engineering, Federal University of São Carlos (UFSCar), Campus of Sorocaba, Rodovia João Leme dos Santos, km 110, Sorocaba, SP, Brazil

[2] Cerema, BPE Research Team, 46, Rue St Théobald, L'Isle d'Abeau F-38080, France

[3] Institute of Sciences and Engineering, São Paulo State University (UNESP) - Campus of Itapeva, Rua Geraldo Alckmin, 519, Itapeva, SP, Brazil

[4] Instituto de Ciencia y Tecnología del Carbono (INCAR-CSIC), Francisco Pintado Fe, 26, Oviedo 33010, Spain

[5] Department of Environmental Sciences, Federal University of São Carlos (UFSCar) – Campus of Sorocaba, Rodovia João Leme dos Santos, km 110, Sorocaba, SP, Brazil

Published online: 27 August 2026

Graphical Abstract

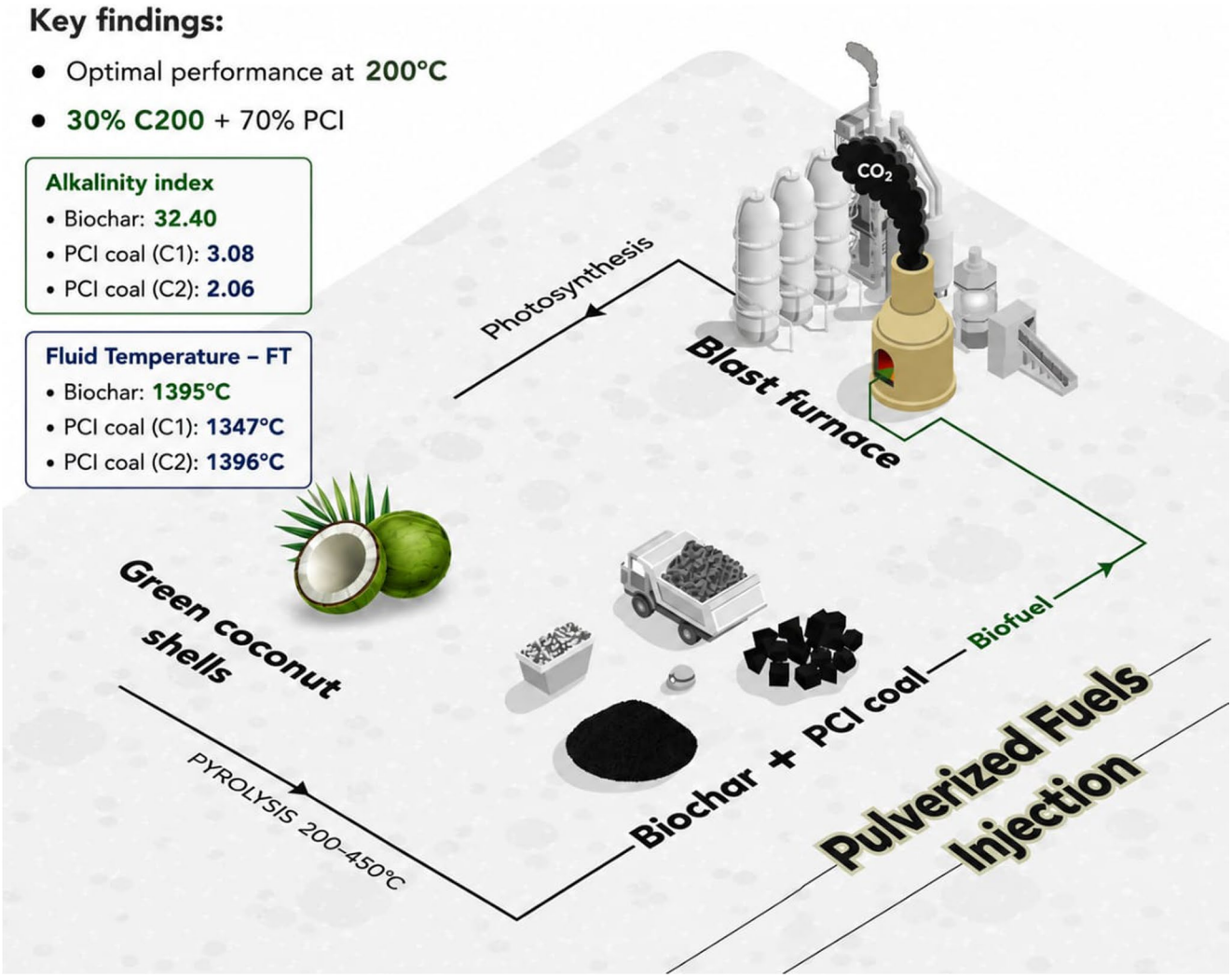

Keywords Thermogravimetric Combustion Behavior · Steelmaking · Pyrolysis · Biomass · Ash

Introduction

The ironmaking process is known for its negative environmental impact due to the substantial emissions of greenhouse gases (GHGs) during its operation [1]. In this context, reducing emissions from ironmaking is directly aligned with the United Nations Sustainable Development Goals (SDGs), particularly SDG 9 (Industry, Innovation and Infrastructure) and SDG 13 (Climate Action) [2]. As global efforts to combat climate change intensify, ironmaking must seek innovative ways to reduce its carbon footprint while maintaining efficiency in blast furnace (BF) operations. One promising solution lies in the partial replacement of fossil fuels with a renewable carbon source, such as biochar, a carbonaceous material derived from biomass pyrolysis [3, 4].

Among potential feedstocks, coconut shells stand out as a relevant residue due to both their abundance and the environmental impacts associated with their inadequate disposal, including methane emissions, environmental pollution, vector proliferation, and reduced landfill lifespan [5–7]. Coconut shell waste is characterized by slow decomposition and is often subjected to inadequate disposal practices. In tropical and subtropical countries, approximately 90% of coconut biomass is discarded as refuse, openly burned, or accumulated in waste ponds, which contributes to environmental degradation [8]. These practices also result in increased municipal maintenance costs and place additional pressure on waste management systems [7]. These issues underscore the urgency of developing sustainable strategies for coconut shell valorization, transforming a problematic

waste into a renewable carbon source suitable for industrial applications [9].

Although raw biomass is unsuitable for direct use in blast furnaces, biochar can be processed and utilized as a pulverized auxiliary fuel within blast furnace injection systems, leveraging existing pulverized coal injection (PCI) technology [10]. This adaptation, known as Bio-PCI, offers a sustainable pathway to reducing CO_2 emissions, optimizing resource utilization, and promoting a circular economy by repurposing agricultural and forestry residues [11, 12]. In countries like Brazil, where biomass availability is abundantly available, this approach has the potential to revolutionize iron production by making it more environmentally and economically sustainable [13].

This technology is particularly relevant as the steel industries transitions toward low-carbon production methods, and its implementation has intensified due to its compatibility with existing PCI systems and the possibility of partial fossil fuel replacement without significant process changes [14, 15]. In Brazil, companies including the Steel Mill of Pará (USIPAR) have conducted experiments employing Bio-PCI technology. The charcoal used for the studies was obtained from the carbonization of açaí seeds, a residue present in abundance in the North region [16]. Previous studies have focused primarily on the physicochemical characterization of biochar, providing a fundamental understanding of its properties, but with limited emphasis on its practical application in industrial systems [12, 17].

Furthermore, the influence of biochar properties on combustion behavior, ash-related issues, and blending performance with PCI coal remains insufficiently explored. This lack of integrated evaluation represents a key research gap in the literature [18]. In this context, the present study aims to address these limitations by investigating the physicochemical properties and combustion behavior of biochar produced from green coconut shells at different pyrolysis temperatures. In addition, this work evaluates the performance of biochar–coal blends, with emphasis on combustion characteristics and ash-related parameters relevant to blast furnace operation. The novelty of this study lies in combining material characterization with combustion analysis and blending evaluation to assess the feasibility of coconut shell-derived biochar as a partial substitute for PCI coal.

Experimental Section

Materials

The raw biomass used in the experiments consisted of green coconut shells (*Cocos nucifera* L.), collected in the city of Sorocaba, São Paulo. The chemical composition and fuel properties of the coconut shell biomass, including 34.36wt% lignin, 30.87wt% cellulose, 30.01 wt% hemicellulose and a bulk density 0.32 g/cm^3, were obtained from a previous study conducted by the authors [19]. The raw biomass was manually cut, weighed, and dried according to the ASTM E871-13 protocol using a Marconi MA 35 air circulation oven. The dried biomass was then milled using a Willey knife mill (Marconi, model MA-340). The biomass preparation process is illustrated in Fig. 1. Subsequently, the milled coconut shells, with a particle size < 0.84 mm, were used for biochar production at laboratory scale, as shown in Fig. 1D.

Two mineral coals, C1 and C2, with particle sizes smaller than 0.212 mm of different qualities were selected for this study. C1 and C2 were of Russian and Colombian origin, respectively. Both coals are commonly used as pulverized coal injection (PCI) coals. C1 was combined with chars in different ratios to produce blends and C2 was included for comparative purposes. The preparation was carried out at INCAR-CSIC and more detailed description of the procedure applied to prepare the coal and of the materials used can be found elsewhere [20].

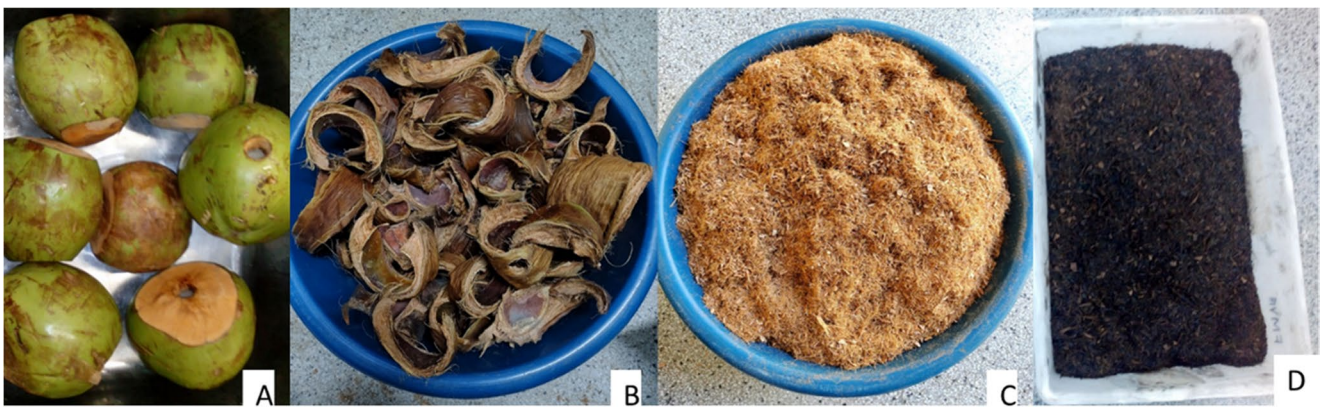

Fig. 1 (**a**) green coconut shells, (**b**) chopped and dried coconut shells, (**c**) milled coconut shells and (**d**) biochar C200 sample

Biochar Production

Biochar was produced at four different pyrolysis temperatures (200, 250, 350, and 450 °C) with a residence time of 6 hours after reaching the target temperature. Approximately 3 kg of the sample, with a particle size smaller than 1.19 mm was heated in a muffle furnace (Jung brand model 0212) to the desired pyrolysis temperature at a heating rate of 20 °C min^{-1} under low-oxidation conditions (oxygen content <1 vol%) [17]. The nomenclature used for the biochar is as follows: follows the pattern 'C' followed by the pyrolysis temperature, for example C200. Mass yield (%) was calculated (with respect to the dry mass of the original sample) on a dry basis using Eq. 1, as follows as follows:

$$Mass\ yield = \frac{m_{biochar}}{m_{raw\ biomass}}\ x\ 100 \quad (1)$$

where $m_{biochar}$ denotes the mass of the biochar and $m_{raw\ biomass}$ denotes the dry mass of the raw biomass.

Materials Characterization

For the biochar samples, proximate analysis was performed according to ASTM D1762-13. For PCI coal, ASTM D7582-15 was used to determine volatile matter and ash content. Elemental analysis (C, H, and N) was conducted using a LECO CHN-2000 in accordance with ASTM D5373. Sulfur **content was measured** using a LECO S-632 (ASTM D4239), and oxygen was determined using a LECO VTF-900. Based on the elemental concentrations, H/C and O/C ratios were calculated to assess the structure and reactivity of the carbonaceous materials. The higher heating value (HHV) was determined using a bomb calorimeter (IKA model C200). All analyses were performed in triplicate. The main characteristics of the materials are presented in Table 1.

For inorganic matter analysis, the chemical composition of the ash was determined by X-ray fluorescence (XRF) following ASTM D4326-04. X-ray fluorescence (XRF) following ASTM D4326-04. The sample preparation procedure was carried out as follows: (i) biochar and PCI coal samples were ashed separately at 815 °C using a heating rate of 7 °C min^{-1}; (ii) 0.5 g of ash was mixed with 9 g of lithium tetraborate/lithium metaborate flux (66:34 ratio, Equilab EQF-TML 66:34); (iii) the mixture was fused at 1100 °C for 8 min in a fusion furnace (PERLX'3, Philips) to obtain a homogeneous glass disk; and (iv) the fused sample was analyzed using an SRS 3000 Bruker spectrometer.

The mineral composition of the samples was further evaluated using the alkalinity index (AI), which represents the ratio of basic to acidic oxides in the ash, as defined in Eq. 2.

$$AI = \frac{[Fe_2O_3] + [CaO] + [MgO] + [K_2O] + [Na_2O]}{x\ ash\ (\%)}, \quad \frac{[SiO_2]+[Al_2O_3]}{} \quad (2)$$

The basic oxides (Fe_2O_3, CaO, MgO, K_2O and Na_2O) generally act as catalysts, whereas acidic oxides (SiO_2 and Al_2O_3) act as inhibitors [20, 21].

Ash fusibility temperatures (AFTs) were determined after preparing biochar and PCI coal ashes in a muffle furnace according to the UNE 32,004 standard method. The AFTs were measured in an oxidizing atmosphere (air) following the ASTM D1857-87 standard using an ash fusibility auto-analyzer (LECO AF700). During the analysis, the ash cone, with standardized geometry, was heated up to 1550 °C at a heating rate of 8 °C min^{-1}. The evolution of the cone shape was recorded using a video camera. An automatic detection system identified and recorded the initial deformation temperature (IT), softening temperature (ST), hemispherical temperature (HT), and fluid temperature (FT) with an

Table 1 Main characteristics of materials injection used in this study

Materials	VM[db, a] (wt%)	Ash [db] (wt%)	FC [db] (wt%)	HHV [db] (MJ/kg)	C [db] (wt%)	H [db] (wt%)	N[db] (wt%)	S [db] (wt%)	O [db] (wt%)	MY[b] (%)
Coconut shells	75.5	2.9	21.6	18.7	39.4	4.3	0.7	0.1	52.6	-
C200	45.3	8.0	46.7	22.8	60.6	3.8	1.4	0.1	25.2	40.5
C250	38.5	10.3	51.2	22.8	62.2	3.6	1.5	0.1	21.4	36.3
C350	35.3	12.7	52.0	23.7	66.3	3.3	1.5	0.1	16.8	30.3
C450	22.0	12.7	65.3	25.9	73.8	2.5	1.3	0.1	10.5	24.9
C1	20.9	9.5	69.6	31.7	79.5	3.9	2.3	0.3	4.6	-
C2	40.6	7.0	52.4	27.9	68.5	4.8	1.8	0.7	17.2	-
C3*	36.4	6.7	56.9	32.1	77.7	4.1	1.8	0.3	9.5	-

* From literature [26]

[db] dry basis

[a] Volatile Matter

[b] Biochar mass yield

accuracy of ± 1 °C. The reported AFTs represent the average values of two independent measurements.

The combustion behavior of the biochar was analyzed using thermogravimetric analysis (TGA). The analysis was performed using a TA Instruments SDT 2960 thermobalance. Approximately 10 mg of sample, with a particle size below 0.212 mm, was heated under an oxidative atmosphere of synthetic air (flow rate of 100 mL min^{-1}) from room temperature to 900 °C at a heating rate of 10 °C min^{-1}. The temperature corresponding to the maximum mass loss (Tmax), the mass yield at Tmax, the maximum mass loss rate (DTGmax) and the residue obtained at 900 °C were determined from the TG data.

Quality of Injection Materials

Parameters such as the combustion indices (FR, CI, and VI) were employed to identify a suitable biochar alternative to PCI coal. These indices are widely used in the literature to evaluate the combustion behavior and suitability of solid fuels for PCI applications, as they are derived from proximate analysis and reflect fuel reactivity and ignition characteristics [15, 22] Combustion indices were calculated using the results of the proximate analysis [17]. These parameters include the fuel ratio – FR (Eq. 3), combustibility index - CI (MJ/kg) (Eq. 4) and volatile ignitability – VI (MJ/kg) (Eq. 5). Solid fuels having FR values in the range 0.5 to 2.0, CI values ranging between 12 and 23 MJ/kg; and VI values of at least 14.5 MJ/kg are recommended in the literature for PCI applications [23]. Where FC is fixed carbon, VM is volatile matter and MC is moisture content all terms in percent dry basis (db).

$$FR = \frac{FC_{db}}{VM_{db}} \tag{3}$$

$$CI = \frac{HHV_{db}}{FR} \times (115 - Ash_{db}) \times \frac{1}{105} \tag{4}$$

$$VI = \left[\frac{HHV_{db} - 0.338FC_{db}}{VM_{db} + MC_{db}}\right] \times 100 \tag{5}$$

The combustion rate was evaluated based on the TG analyses, which were carried out using a TA Instruments SDT 2960 thermobalance. Approximately 10 mg of sample, biochar and PCI coals, with a particle size smaller than 0.212 mm were heated under a N_2 flow of 100 mL/min from room temperature to 1010 °C at a rate of 10 °C/min. A nitrogen flow was maintained during this stage to prevent oxidation and to remove the pyrolysis products. Once the temperature was stabilized, the carrier gas was switched to synthetic air using a flow of 100 mL/min for 20 min or until a conversion degree greater than 90% was reached. The conversion (X) and combustion rate (DTGmax) were calculated from the TG data using Eqs. 7 and 8, respectively:

$$F_{ash} = \frac{100}{100 - m_{ash}} \tag{6}$$

$$X\ (\%) = \frac{m_0\ (g) - m_i\,(g)}{m_0\ (g) - F_{ash}} \tag{7}$$

$$DTG\,(\%/min) = \frac{dX}{dt} \tag{8}$$

Where m_0 represents the initial mass of the sample, m_i the mass at time t and m_{ash} ash mass. Based on the results, the C200 biochar was selected and mixed with PCI coal C1 in percentages of 10%, 30%, and 50% to study the effect of biochar addition on the behavior of PCI coals using thermogravimetric analysis under isothermal heating at 1000 °C.

Statistical Analysis

The experimentally obtained data were statistically evaluated using the software R-3.5.1. The analysis of variance (ANOVA) and Tukey's multiple range tests (5% probability) were also conducted.

Results and Discussion

Figure 1 shows the dried and crushed coconut shells, before and after pyrolysis at a temperature of 200 °C. The resulting biochar exhibited physical characteristics such as moisture content lower than 2 wt%, particle size smaller than 16 mesh and exhibited high grindability. This result was expected, as it is widely known that powdered biochar cannot be charged into the BF along with iron ore. However, an application in the reactor could be as an auxiliary fuel using the Bio-PCI technology, where its physical characteristics become advantageous, since biochar is easy to grind or pulverize [24]. The following sections discuss the physical and chemical characteristics of biochar and compare them with the characteristics of PCI coals used in the steel industry to assess the feasibility of this application.

For the production of 1 kg of each type of biochar (C200, C250, C350, and C450), considering the yields presented in Table 1, a total of 60 kg of fresh green coconut shells was used. After the drying process, the initial moisture content of the raw material on a wet basis was calculated. The results showed that the raw coconut shells had a moisture content of 79%.

Characterization of Biochar and PCI Coals

The results of the proximate analysis, elemental composition, and higher heating value (HHV) of the materials injection are shown in Table 1.

Table 1 shows that coconut shells exhibit energetic characteristics typical of a lignocellulosic biomass, such as high volatile matter and low fixed carbon content. Biomass materials generally display these characteristics, with volatile matter being the largest fraction of the material's constituents. These typical characteristics of the raw biomass are the main drawback when the material is intended for direct application in the blast furnace (BF). The values observed are consistent with those reported in the literature for coconut shells (72–77 wt% VM, 0–2 wt% ash and 18.25 MJ/kg HHV) [25, 26].

The conditions of the pyrolysis process have a substantial impact on the physicochemical properties and yield of the resulting products [27]. Consequently, optimizing process parameters is essential for improving biomass quality. As a thermochemical process, pyrolysis is highly influenced by temperature, Yang et al. highlight that peak pyrolysis temperature is the most influential parameter among all process conditions [28]. Indeed, when comparing the coconut shells with the resulting biochars, it was observed that the energetic characteristics were improved progressively. As shown in Table 1, pyrolysis temperature directly affects carbon content (ranging from 39.4% to 73.8%) and ash content (from 2.9% to 12.7%), while volatile matter decreases as temperature increases (from 75.5% to 22.0%). With the rise in pyrolysis temperature, there was also a statistically significant increase in the HHV of the biochars. The obtained biochars exhibited slightly lower HHV than the eucalyptus charcoal fines traditionally used in the Brazilian steel industry (30.97 MJ/kg to 31.63 MJ/kg) [29].

The main alterations in the properties of biochar result from the volatilization and decomposition of the biomass constituents, resulting in mass loss. Therefore, increasing the pyrolysis temperature also causes a decrease in the mass yield. The results of the proximate and elemental analyses can be used to optimize the operational conditions of the pyrolysis process, aiming at the production of higher-quality biochar [30]. Based on the HHV and mass yield results, the C200 biochar exhibited the highest mass yield, while no statistically significant differences in HHV were observed among biochars produced at temperatures up to 350 °C. However, although higher pyrolysis temperatures led to increased fixed carbon and carbon content, they were also associated with higher ash content and lower mass yield. The selection of C200 for the blending experiments was therefore based on a balance between yield, energy content, and ash-related properties, as well as its closer similarity to PCI coal in terms of ash content. Other parameters, including combustion indices and ash composition, should also be considered when selecting a biochar suitable for use as a BF auxiliary fuel.

Regarding ash content, the raw biomass exhibited the lowest value (< 3.0%) among all the injection materials (Table 1). It was observed that increasing the pyrolysis temperature, there was also a statistically significant increase in the ash content. This behavior can be explained by the removal of organic matter during pyrolysis, increasing the proportion of mineral elements (non-volatile) in the distribution of constituents in the biochars [28]. The ash present in biomass is an inert material; therefore, its content increases when the rest of the biomass undergoes decomposition during pyrolysis conditions. Furthermore, in Table 1, it can be observed that the biochars had ash content ranging from 8.0% to 12.7%. The C200 biochar recorded the lowest ash content, falling within the range presented by the reference PCI coals, which ranged between 6.7% and 9.5%.

At the bottom of the BF, in front of each tuyere, the combustion of the pulverized auxiliary fuel takes place, generating heat and enriching the gas with carbon monoxide, which rises through the shaft and reduces the iron burden, resulting mainly in the formation of liquid iron and carbon dioxide [31]. The composition of the ashe plays a crucial role in the success of this process and the overall performance of the BF. Therefore, during combustion, important products, in addition to CO, include chlorides, sulfates, carbonates, and alkali silicates, formed through reactions between inorganic species that must be controlled due to the formation of fouling and slagging [32–34]. To assess this, the ash chemical composition, alkalinity index (AI), and ash fusibility temperatures (AFTs) of the injection materials were analyzed, as shown in Tables 2 and 3.

Table 2 shows that the ash derived from biochar exhibited a markedly different chemical profile compared to that of the PCI coal ashes. The biochar ashes were characterized by high contents of alkali and alkaline earth oxides, and low levels of SiO_2 (11.7%) and Al_2O_3 (< 0.01%), when compared to the PCI coal ashes. Such composition has been associated in the literature with increased slagging and fouling tendencies due to the presence of alkali species [35–39]. Potassium is the dominant source of alkali in most biomass fuels and plays a central role in reacting with silica to form alkali silicates that can melt or soften at relatively low temperatures (< 700 °C) [40]. In contrast, the PCI coals exhibited a more silica and alumina-rich composition. C1 contained 47.4% SiO_2 and 24.2% Al_2O_3, while C2 contained 35.8% SiO_2 and 33.9% Al_2O_3. These oxides are known to contribute to the refractory nature of ash, raising its melting point and improving slag resistance [34, 39, 41].

Table 2 Ash composition and alkalinity index of the materials

	Biochar C200	C1	C2
Na_2O (%, db)	4.8	0.8	7.7
MgO (%, db)	8.8	2.9	1.7
AL_2O_3 (%, db)	<0.01	24.2	33.9
SiO_2 (%, db)	11.7	47.4	35.8
P_2O_5 (%, db)	8.2	0.7	0.1
K_2O (%, db)	39.7	3.5	0.9
CaO (%, db)	10.0	6.7	6.6
TiO_2 (%, db)	0.1	0.8	1.1
Fe_2O_3 (%, db)	0.7	9.2	3.5
SO_3 (%, db)	3.1	2.9	7.5
MnO (%, db)	0.1	0.1	<0.001
ZnO (%, db)	0.1	0.0	0.0
SrO (wt %, db)	0.0	0.2	0.0
V_2O_5 (%, db)	<0.001	<0.001	0.3
Cr_2O_3 (%, db)	<0.001	<0.001	0.0
NiO (%, db)	<0.001	0.0	0.1
ZrO_2 (%, db)	12.6	<0.001	<0.001
AI (%)	32.40	3.08	2.06

[db] dry basis

AI alkalinity index

Table 3 Ash fusibility temperatures in an oxidizing atmosphere

AFT_S	Maximum		
	Biochar	C1	C2
Initial deformation Temperature - IT (°C)	1266	1260	1184
Softening Temperature - ST (°C)	1318	1285	1268
Hemispherical Temperature - HT (°C)	1355	1319	1294
Fluid Temperature - FT (°C)	1395	1347	1396

A particularly notable parameter is the alkalinity index (AI), which reflects the balance between basic (low-melting) and acidic (high-melting) oxides. The biochar exhibited a very high AI of 32.40, compared to 3.08 for C1 and 2.06 for C2. High AI values are commonly used as indicators of increased slagging propensity and potential ash-related operational issues in high-temperature systems [33, 39, 42]. Therefore, the elevated AI observed for the biochar suggests a higher likelihood of slagging and fouling under certain operating conditions. However, it should be noted that these assessments are based on ash composition and empirical indices, and the actual behavior in blast furnace conditions may vary depending on process parameters and should be further validated experimentally.

The results indicate that the biochar ash, due to their composition and consequently high reactivity, may cause issues in subsequent reactions between the reducing agent and the iron burden, as well as in slag formation. Blending C200 biochar with a higher-quality PCI coal, such as C1, may mitigate these effects by lowering the overall alkalinity index and increasing the proportion of refractory oxides in the ash, potentially reducing slagging and refractory degradation [43–45]. The ash fusibility temperatures (AFTs) provide important insight into the behavior of solid fuel ash in high-temperature processes such as those in BFs. Therefore, AFTs can be used as parameters for evaluating the performance of solid fuels in BFs. The results of the ash fusibility temperatures (AFT_S) are presented in Table 3.

AFTs indicate the thermal behavior and melting progression of ash under oxidizing conditions. The effect of compositional differences (Table 2) is evident in the ash fusibility behavior, as shown in Table 3. Biochar exhibited higher AFTs at all key stages compared to the PCI coals, C1 and C2, particularly the latter, whose IT was as low as 1184 °C and HT was 1294 °C. This apparent contradiction, high alkali content yet high AFTs, suggests that factors beyond simple AI are influencing fusibility. One hypothesis is that the presence of magnesium oxide (MgO, 8.8%) and zirconium oxide (ZrO_2, 12.6%) in the biochar ash may contribute to the formation of higher-melting phases that stabilize the ash matrix, counteracting the fluxing effects of K_2O and Na_2O and delaying deformation [34, 46].

Thermogravimetric Analysis (TGA)

The thermal decomposition of the produced biochars was studied using thermogravimetric (TG) and derivative thermogravimetric (DTG) curves, which provide a correlation between the materials mass loss and temperature. The thermal characteristics of the studied biochars is illustrated in the TG curves shown in Fig. 2.

The thermal behavior of raw coconut shell biomass is divided into four main stages of decomposition stages, evaporation of moisture or free water, that occurs between room temperature and 100 °C, hemicellulose at a temperature range of 250–323 °C, cellulose at 390 °C and lignin that occurs at temperatures above 400 °C [47]. For the biochars, these events are less pronounced as the pyrolysis temperature increases, decomposing part of the natural constituents of the coconut shell. In the TG curves, starting from room temperature, an initial mass loss was observed until approximately 150 °C, which can be attributed to residual moisture [48]. Between 200 and 600 °C, there was a rapid mass loss due to the release of volatile matter, which, under oxidizing conditions, ignites and burns. After the release of volatiles, from 600 °C onwards, there was a slow mass loss as the residual carbon fully decomposed into ash at 900 °C [49].

As evidenced by the results of the proximate analysis, pyrolysis temperature is a key parameter for the quality of the biochar. The thermochemical process led to the partial thermal decomposition of the biomass constituents (lignin, cellulose, and hemicellulose), resulting in significant changes

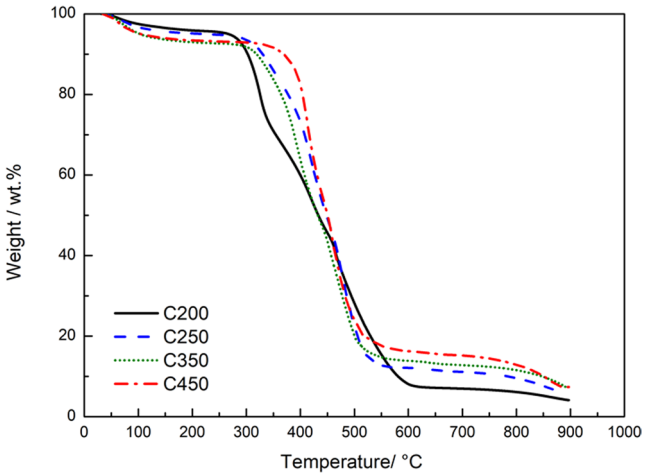

Fig. 2 Comparative analysis of the TG curves of the produced biochars

in the material's properties. Due to the intrinsic differences in the chemical structures of the biomass constituents, it is possible to distinguish the thermal decomposition of each component through thermogravimetric techniques [50].

Using derivative thermogravimetry (DTG), it is possible to observe the temperatures at which the main decomposition stages occur, as well as the rates of maximum degradation (DTG_{max}) in the studied materials can be identified. The peaks or mass losses observed can be attributed to the decomposition of specific biomass constituents. According to Zhou et al., the thermal decomposition of biomass follows the order hemicellulose > cellulose > lignin; however, the decomposition of these compounds occurs simultaneously, complicating their identification [50]. Table 4 presents the biochar yield at each decomposition stage, the temperatures of maximum mass loss, and the residue remaining at 900 °C.

Table 4 TG / DTG values of biochar samples

		Material			
		C200	C250	C350	C450
	Mass (wt.%)[a]	80.0	88.5	87.7	
1° stage (Hemicellulose)	Tmax (°C)[b]	325	338	332	*
	DTG max[c] (wt.%/min)	12.0	3.9	4.1	*
	Mass (wt.%)[a]	53.4	64.3	69.3	75.4
2° stage (Cellulose)	Tmax (°C)[b]	422	419	390	410
	DTG max[c](wt.%/min)	6.4	11.2	11.4	18.2
	Mass (wt.%)[a]	41.2	34.9	42.5	46.6
3° stage (Lignin)	Tmax (°C)[b]	464	478	452	456
	DTG max[c](wt.%/min)	10.9	14.2	11.14	20.4
	Ash (%)[d]	4.1	8.7	6.9	7.3

* Not detected[a] Mass (wt.%), biochar yield at specific temperature (Tmax)[b] Tmax, temperature for maximum mass loss[c] DTGmax, maximum mass loss rate[d] Ash at 900 °C

The difference in ash content observed between Tables 1 and 4 can be attributed to the specific conditions associated with each analytical method, particularly sample preparation procedures. In the case of thermogravimetric analysis, the use of smaller sample masses may lead to a reduction in impurities, resulting in lower measured ash content.

Figure 3 illustrates the DTG curves of the studied biochars. It is important to highlight that the DTG curves use different scales on the y-axis to better visualize the peaks associated with the decomposition of hemicellulose, cellulose and lignin. However, the difference has an impact on the reading of the reaction rates, which are higher for C450 compared to C200.

The initial mass loss around 100 °C, attributed to water evaporation that was not removed during drying, was not considered a degradation stage of the material. The thermal decomposition of all studied biochars occurred in three stages, showing three well-defined peaks in the DTG curves, which can be attributed to the degradation of the main components of biochar.

According to Zhou et al., the thermochemical conversion of hemicellulose mainly occurs in the temperature range of approximately 200–350 °C [50]. In the C200 biochar sample, the peak in this range represents the highest mass loss, occurring with a maximum mass loss rate of 12%/min at 325 °C (Fig. 3A). When comparing the biochars in this first stage, a reduction in the intensity of this peak is observed, indicating lower mass loss due to the progressive decomposition of hemicellulose with increasing pyrolysis temperature. The absence of this peak in the C450 biochar likely indicates the complete elimination of hemicellulose at this pyrolysis temperature (Fig. 3D).

Two additional stages were observed after the first peak, likely corresponding to the decomposition of cellulose and a portion of lignin. The thermal decomposition of cellulose mainly occurs between 300 and 400 °C [50]. The produced biochars showed mass loss between 390 and 422 °C, which is related to the decomposition of cellulose. Lignin typically undergoes a progressive and partial decomposition during pyrolysis starting from around 200 °C, but its main degradation in the third stage occurred at higher temperatures, "approximately 450 °C [50, 51].

In PCI application within the BF, there is practically no heating rate. The materials are injected into the furnace, which reaches a temperatures of approximately 2000 °C, resulting in the almost instantaneous combustion of the materials [21]. Therefore, while the dynamic thermogravimetric analysis provides valuable insights into the thermal behavior of the biochar and enables comparisons of fuels, its application in the actual PCI process should be

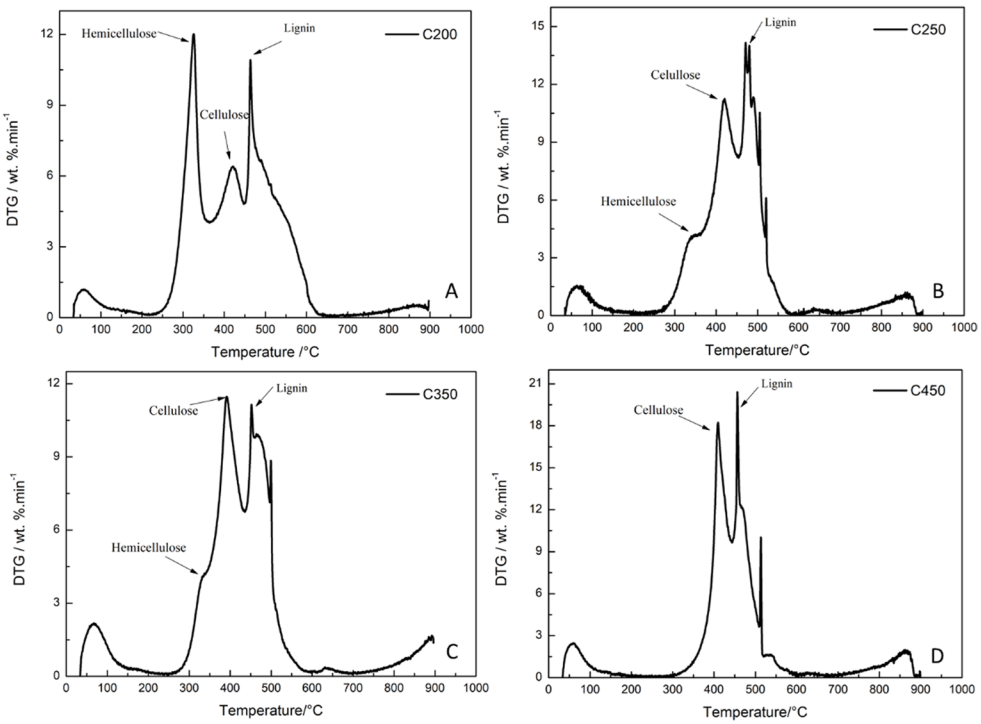

Fig. 3 Comparative analysis of the DTG curves of the produced biochars at different pyrolysis temperatures: (**a**) C200, (**b**) C250, (**c**) C350, and (**d**) C450

done with caution and may require further investigation and experimentation to account for the differences in conditions. Isothermal thermogravimetric techniques are commonly used to investigate the combustion process in the actual BF.

Biochar Quality Determination

Table 5 presents the combustion index values, along with the H/C and O/C ratios, for the raw biomass, biochars produced at different pyrolysis temperatures, PCI coals (C1 and C2), and a reference PCI coal from the literature [52]. To compare the suitability of the materials for injection, the combustion index and the atomic ratio H/C and O/C were used. These parameters were calculated based on the results of the proximate and elemental analyses.

The two selected mineral coals, C1 and C2, are classified as pulverized coal injection (PCI) coals. These coals are used exclusively as fuel in BF due to their non-coking nature, meaning they be used to produce metallurgical coke. The determination of the combustion indices allowed verifying which biochar met the criteria for a PCI coal, allowing the selection of the most suitable one for use as a pulverized solid fuel in the BF.

The results indicate that raw coconut shells do not meet the values recommended by the combustion indices and therefore, do fulfill the specifications required for PCI coal in BF operations. However the biochars C200, C250, and C350 satisfy all recommended thresholds for l combustion indices and display values close to the PCI coals C2 and C3.

Table 5 Combustion index values, H/C and O/C ratios

Material	FR[a]	CI[b] (MJ/kg)	VI[c] (MJ/kg)	H/C[d]	O/C[d]
Coconut shell	0.3	69.6	15.1	1.1	1.3
C200	1.0	22.8	15.9	0.6	0.4
C250	1.3	17.3	14.6	0.6	0.3
C350	1.5	15.6	17.1	0.5	0.3
C450	3.0	8.5	17.2	0.3	0.1
C1	3.3	9.5	39.3	0.5	0.1
C2	1.3	22.2	25.1	0.7	0.3
C3*	1.6	21.2	35.2	0.5	0.1

* Calculated from proximate analyses by [52]

[a] Fuel ratio

[b] Combustibility index

[c] Volatile ignitability

[d] Atomic ratio

These findings suggest that C200 e C350 biochars could be used partially as solid fuels in the BF. Nonetheless, it should be noted that higher pyrolysis temperature leads to reduced mass yield. Therefore, when prioritizing the mass yield, the biochar C200 (produced at 200 °C) appears to be the most suitable option among the biochars produced.

The C450 biochar (produced at 450 °C) proved unsuitable for application, as it showed a fuel ratio FR 50% than the recommended threshold while simultaneously exhibiting a low combustion index (CI). This is attributed to the higher pyrolysis temperatures, which promote extensive biomass decomposition, significantly increasing the fixed carbon content while reducing volatile matter.

Under condition, according to Singh et al., higher FR values lead to an increase in the unburned portion of the fuel in the BF. FR values greater than 2 can cause ignition and flammability issues during application [53]. The CI index can be used to assess the compatibility of the material for co-combustion with coal [54, 55]. Thus, the low CI value of C450 suggests that this biochar is unsuitable for co-combustion with mineral coal.

The results of H/C and O/C ratios showed that the raw coconut shell had the highest H/C and O/C atomic ratios (> 1.0) among all the materials studied. As expected, pyrolysis led to a decrease in the H/C and O/C atomic ratios due to the removal of hydrogen and oxygen from the biomass structure, consequently increasing the carbon content in the resulting biochars.

Influence of the Biochar Addition on PCI Coal Quality

To study the combustion behavior of the materials under conditions similar to those in the BF, as well as the effect of adding biochar to PCI coals, thermogravimetric analyses were performed under isothermal heating at 1000 °C. In this analysis, the mass loss was converted to the dimensionless conversion fraction by normalizing with respect to the total mass loss over the experiment. From the conversion curves (X), the combustion rates (DTG) were calculated, where the value of DTGmax is associated with the maximum combustion rate of the material. From the TG data the following parameters were derived (see Table 5): time and combustion rate for a 25 and 50% conversion ($t_{25\%}$, $t_{50\%}$, $DTG_{25\%}$ and $DTG_{50\%}$), time for maximum combustion rate (t_{DTGmax}), maximum combustion rate (DTG_{max}) and conversion at maximum combustion rate (X_{DTGmax}). Three of biochar/coal blends were prepared by adding C200 biochar to C1 mineral coal in different percentages, as shown in Table 6.

The conversion and combustion rate curves of the biochar and blends, as determined by thermogravimetric analysis, are presented in Fig. 4. In Fig. 4C, it can be observed that there were no significant differences among the biochars during the conversion process. However, under isothermal heating, it was noticed that the rate of volatile emission ends earlier in the biochars compared to the PCI coals. These results are consistent with the material composition. As observed in the ash composition, the biochars exhibited a higher content of basic oxides (Fe_2O_3, CaO, MgO, K_2O, and Na_2O), which are known to affect reaction rates and act as catalysts during combustion, resulting in an increase in combustion rates (DTGmax) [34].

According to the data in Table 6, compared to PCI coals, the biochars exhibited higher combustion rates (DTGmax) ranging from 29.9 and 31.7%/min and shorter reaction times (t_{DTGmax}) between 3.8 and 5.1 min. However, when the C200 biochar was blended with the C1 coal, the parameters were improved, reducing the combustion rates and increasing the reaction times in the blends. Thus, the results indicate that a mixture composed of 30% C200 and 70% C1 exhibits thermal behavior suitable for PCI applications, showing characteristics similar to PCI injection coals. This finding is significant for the steel industry since injecting 30% biochar, considered a carbon-neutral source, could significantly reduce CO_2 emissions from the process.

Table 6 Parameters derived from the isothermal thermogravimetric techniques

Material	$X_{25\%}$ [a]		$X_{50\%}$ [b]		Maximum		
	$DTG_{25\%}$ (%/min)	$t_{25\%}$ (min)	$DTG_{50\%}$ (%/min)	t_{50} (min)	DTG_{max} [c] (%/min)	t_{DTGmax}(min)	X_{DTGmax}(%)
C200	21.6	2.8	28.7	3.8	30.1	4.3	63
C250	21.3	2.8	29.2	3.8	31.7	4.4	69
C350	22.6	2.4	30.2	3.4	31.4	3.8	63
C450	19.0	3.0	26.1	4.1	29.9	5.1	78
C1	13.3	3.9	17.2	5.5	18.6	6.9	76
C2	14.2	3.6	17.9	5.1	18.2	5.5	57
50%C200	17.1	3.3	21.8	4.6	23.6 A	5.4 A	69
30%C200	15.2	3.7	19.5	5.1	20.1 B	5.6 A	60
10%C200	13.4	4.0	16.2	5.6	16.8 C	6.5 B	64

[a] Conversion 25%

[b] Conversion 50%

[c] Maximum combustion rate

Means followed by the same letter, in the column, do not differ statistically from each other, at a significance level of 95% (α = 0.05) in the Tukey test

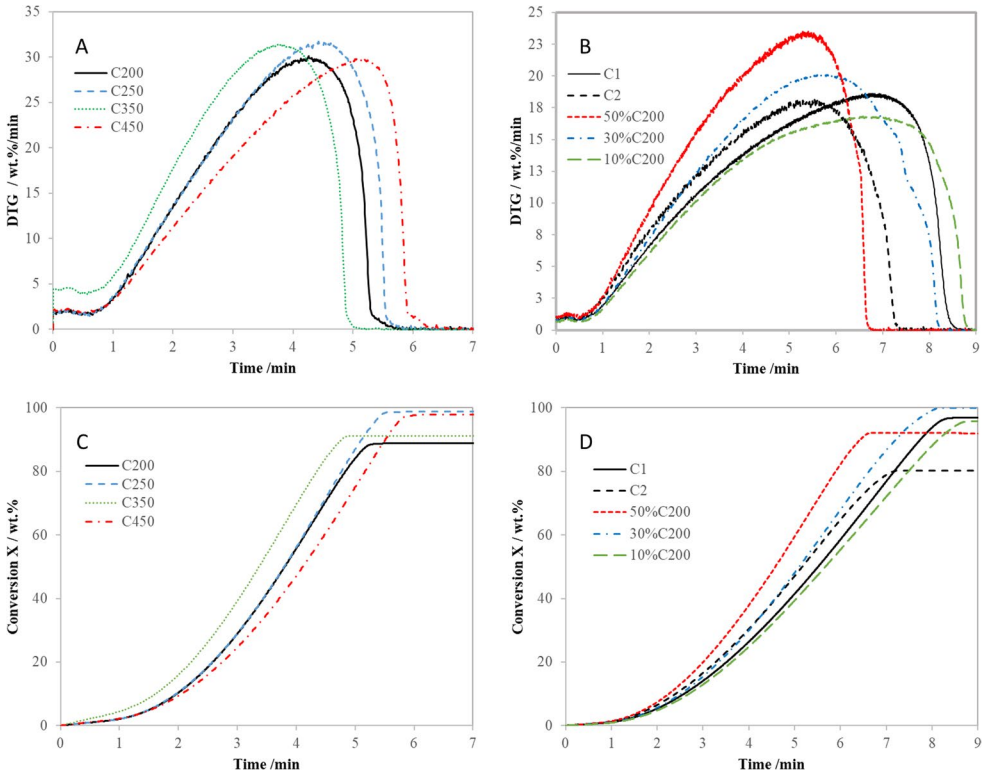

Fig. 4 Combustion rate (DTG) and conversion (X): (**a**) DTG of biochars; (**b**) DTG of blends; (**c**) Conversion of biochar; and (**d**) Conversion of blends

Conclusions

In conclusion, the results showed that the biochar produced at 200 °C (C200) exhibited promising characteristics for use as a solid fuel in the BF, with appropriate combustion indexes and mass yield. Additionally, the C200 biochar demonstrated thermal behavior similar to that of conventional PCI coals used in the industry. Thermogravimetric analysis (TGA) provided valuable insights into the thermal behavior of the biochars, revealing the main decomposition stages of biomass constituents at different temperatures. The biochars exhibited higher combustion rates and shorter reaction times compared to pure PCI coals, indicating easier ignition and volatilization. These results are attributed to the composition of the biochars, which contain a higher amount of basic oxides known to exert a catalytic effect on combustion. The addition of biochar to PCI coal C1 in the mixtures showed promising results, improving thermal behavior and contributing to the reduction of CO_2 emissions. The results indicate that the blend composed of 30%C200 and 70% coal C1 exhibited thermal behavior comparable to that of conventional PCI injection coals, making it a viable alternative for application in the steel industry.

Acknowledgements The authors thank Biomass and Bioenergy research group of UFSCar (Sorocaba campus), and the Instituto Nacional del Carbón, INCAR-CSIC for supporting this project. This study was partially financed by Coordenação de Aperfeiçoamento de Pessoal de Nível Superior - Brazil (CAPES) (Finance Code 001) and National Council for Scientific and Technological Development (CNPq - Process n° 406810/2022-2).

Author Contributions ERDP, DAM e CMSRL escreveram o texto principal do manuscrito. CIC e CB contribuíram com a análise dos dados e revisão crítica do conteúdo. RSR participou da concepção do trabalho, organização dos resultados e redação final. FMY supervisionou o projeto e revisou o manuscrito. Todos os autores revisaram e aprovaram a versão final do manuscrito.

Funding The Article Processing Charge (APC) for the publication of this research was funded by the Coordenação de Aperfeiçoamento de Pessoal de Nível Superior - Brasil (CAPES) (ROR identifier: 00x0ma614).

Data Availability No datasets were generated or analysed during the current study.

Declarations

Competing interests The authors declare no competing interests.

References

1. Campos AMA, Leal A, Salles S, Assis PS (2024) Biomass and energy connected with iron and steelmaking. Tecnol Metal Mater Min 21:e3053. https://doi.org/10.4322/2176-1523.20243053
2. Nations U, Sustainable Development Goals United Nations Department Of Global Communications Guidelines for the Use of the Sdg (2023) Sep., Logo Including the Colour Wheel, and 17 Icons, Accessed: Jul. 11, 2026. [Online]. Available: https://www.un.org/sustainabledevelopment/wp-content/uploads/2023/09/E_SDG_Guidelines_Sep20238.pdf
3. Chen W-H et al (2021) Progress in biomass torrefaction: principles, applications and challenges. Prog Energy Combust Sci 82:100887. https://doi.org/10.1016/j.pecs.2020.100887
4. Li H, Zhao Y, Guo C, Li J (2024) Analysis of technological pathways and development suggestions for blast furnace low-carbon ironmaking. Metals 14(11):1276. https://doi.org/10.3390/met14111276
5. Monroe APR et al (2024) Evaluation of the bioenergy potential of blends (green coconut shells and fish scales) as a feedstock in thermochemical processes for clean energy production. Processes 12(4):710. https://doi.org/10.3390/pr12040710
6. Vieira F et al (2024) Coconut waste: discovering sustainable approaches to advance a circular economy. Sustainability 16(7):3066. https://doi.org/10.3390/su16073066
7. Guerra MA, Iturralde F (2024) Literature Review Of Coconut Shell And Fibers In Pavement Design, *Proceedings of International Structural Engineering and Construction*, vol. 11, no. 1, Mar. https://doi.org/10.14455/ISEC.2024.11(1).MAT-07
8. Yerima I, Umar MA (2025) Investigation of combustion efficiency of coconut shell (*Cocos nucifera*) in an improved stove in comparison with neem wood. J Divers Stud 4(1):68–72. https://doi.org/10.51470/JOD.2025.4.1.68
9. Lestari AND et al (2025) Coconut shell waste reduction through briquette innovation: an environmentally friendly and economic improvement solution. Qardhul Hasan: Media Pengabdian kepada Masyarakat 11(1):75–85. https://doi.org/10.30997/qh.v11i1.17858
10. Campos AMA, Khozhanov N, Assis PS, Tursunbaev K, Masatbayev M (2021) Economic and environmental analyses of biomass torrefaction for injection as pulverized material in blast furnaces. REM Int Eng J 74(4):471–482. https://doi.org/10.1590/0370-44672020740101
11. Abhi TD et al (2023) Challenges and opportunities of agricultural biomass as a replacement for PCI coal in the ironmaking blast furnace: a review. J Sustain Metall 9(3):927–949. https://doi.org/10.1007/s40831-023-00720-2
12. Ibitoye SE et al (2024) An overview of biochar production techniques and application in iron and steel industries. Bioresour Bioprocess 11(1):65. https://doi.org/10.1186/s40643-024-00779-z
13. Wang RQ, Jiang L, Wang YD, Font-Palma C, Skoulou V, Roskilly AP (2024) Woody biomass waste derivatives in decarbonised blast furnace ironmaking process. Renew Sustain Energy Rev 199:114465. https://doi.org/10.1016/j.rser.2024.114465
14. Fan Z, Friedmann SJ (2021) Low-carbon production of iron and steel: Technology options, economic assessment, and policy, *Joule*, vol. 5, no. 4, pp. 829–862, Apr. https://doi.org/10.1016/j.joule.2021.02.018
15. Kim M-W, Ku M-J, Kim J, Kim G-M, Jeon C-H, Lee D-G (2026) Towards Carbon-Neutral Ironmaking: Stepwise Integration of Biocarbon in PCI with Combustion Behavior Characterization and Injection Limit Evaluation, *Engineering*, vol. 59, pp. 215–228, Apr. https://doi.org/10.1016/j.eng.2025.12.004
16. Feliciano-Bruzual C Charcoal injection in blast furnaces (Bio-PCI): CO2 reduction potential and economic prospects. J Mater Res Technol 3(3):233–243. https://doi.org/10.1016/j.jmrt.2014.06.001
17. Durango Padilla ER, Hansted FAS, Luna CMR, de Campos CI, Yamaji FM Biochar derived from agricultural waste and its application as energy source in blast furnace. Renew Energy 220:119688. https://doi.org/10.1016/j.renene.2023.119688
18. Khasraw D, Martin C, Herbert J, Li Z A comprehensive literature review of biomass characterisation and application for iron and steelmaking processes. Fuel 368:131459. https://doi.org/10.1016/j.fuel.2024.131459
19. Durango Padilla ER, Yamaji FM, Romero Luna CM, de Campos CI, Barriocanal C (2025) Replacement of metallurgical coke with Bio-Coke from coconut shells. Energy Fuels 39(37):17859–17868. https://doi.org/10.1021/acs.energyfuels.5c02366
20. Vega MF, Díaz-Faes E, Barriocanal C (2021) Influence of the Heating Rate on the Quality of Metallurgical Coke, *ACS Omega*, vol. 6, no. 50, pp. 34615–34623, Dec. https://doi.org/10.1021/acsomega.1c05007
21. Suo H et al Organic solid waste as sustainable fuels and reducing agents in low-carbon steelmaking technologies. Fuel 392:134825. https://doi.org/10.1016/j.fuel.2025.134825
22. Lee D-G et al Combustion visualization analysis of alternative fuels in the pulverized coal injection raceway through laminar flow reactor. Heliyon 10(17):e36238. https://doi.org/10.1016/j.heliyon.2024.e36238
23. Waheed MA, Akogun OA (2021) Quality enhancement of fuel briquette from cornhusk and cassava peel blends for co-firing in coal thermal plant, *Int. J. Energy Res.*, 45(2):1867–1878. https://doi.org/10.1002/er.5865
24. Liu Y, Shen Y (2021) Modelling and optimisation of biomass injection in ironmaking blast furnaces. Prog Energy Combust Sci 87:100952. https://doi.org/10.1016/j.pecs.2021.100952
25. Hasan MF, Abdul Rahman MR, Nyakuma BB, Muhamad Said MF (2024) Alternatives for inert torrefaction to produce high-quality solid fuel: Review of available techniques, parameters, potentials and challenges, *Biomass Bioenergy,* 182:107108. https://doi.org/10.1016/j.biombioe.2024.107108
26. Ajien A, Idris J, Md Sofwan N, Husen R, Seli H Coconut shell and husk biochar: A review of production and activation technology, economic, financial aspect and application. Waste Manage Research: J Sustainable Circular Econ 41(1):37–51. https://doi.org/10.1177/0734242X221127167
27. Al-Rumaihi A, Shahbaz M, Mckay G, Mackey H, Al-Ansari T A review of pyrolysis technologies and feedstock: A blending approach for plastic and biomass towards optimum biochar yield. Renew Sustain Energy Rev 167:112715. https://doi.org/10.1016/j.rser.2022.112715
28. Yang X et al Effects of torrefaction pretreatment on fuel quality and combustion characteristics of biomass: A review. Fuel 358:130314. https://doi.org/10.1016/j.fuel.2023.130314
29. Massuque J, Roque Lima MD, Müller da Silva PH, de Paula T, Protásio, Trugilho PF (2023) Potential of charcoal from non-commercial Corymbia and Eucalyptus wood for use in the steel industry. *Renew. Energy*, 211:179–187. https://doi.org/10.1016/j.renene.2023.04.061
30. Manatura K et al Optimization of torrefaction parameters for coconut shell using Taguchi method: Impact on torrefaction performances, combustion characteristics, and thermal stability. Therm Sci Eng Progress 57:103137. https://doi.org/10.1016/j.tsep.2024.103137
31. Ji Z et al Resourceful utilization of combustible solid wastes throughout steelmaking processes: Recent progress and prospects. J Clean Prod 449:141696. https://doi.org/10.1016/j.jclepro.2024.141696
32. Anand A, Gautam S, Kundu K, Ram LC Bio-coke: A sustainable solution to Indian metallurgical coal crisis. J Anal Appl Pyrol 171:105977. https://doi.org/10.1016/j.jaap.2023.105977

33. Abioye KJ et al A review of biomass ash related problems: Mechanism, solution, and outlook. J Energy Inst 112:101490. https://doi.org/10.1016/j.joei.2023.101490
34. Adeleke AA et al A comprehensive review on the similarity and disparity of torrefied biomass and coal properties. Renew Sustain Energy Rev 199:114502. https://doi.org/10.1016/j.rser.2024.114502
35. Zhu H, Liao Q, Hu L, Xie L, Qu B, Gao R (2023) Effect of removal of alkali and alkaline earth metals in cornstalk on slagging/fouling and co-combustion characteristics of cornstalk/coal blends for biomass applications. Renew Energy 207:275–285. https://doi.org/10.1016/j.renene.2023.03.022
36. Yao X, Zhao Z, Li J, Zhang B, Zhou H, Xu K Experimental investigation of physicochemical and slagging characteristics of inorganic constituents in ash residues from gasification of different herbaceous biomass. Energy 198:117367. https://doi.org/10.1016/j.energy.2020.117367
37. Lachman J, Baláš M, Lisý M, Lisá H, Milčák P, Elbl P (2021) An overview of slagging and fouling indicators and their applicability to biomass fuels, *Fuel Processing Technology*, vol. 217, p. 106804, Jun. https://doi.org/10.1016/j.fuproc.2021.106804
38. Wu X et al (2022) Ash Deposition and Slagging Behavior of Xinjiang High-Alkali Coal in a 20MWth Cyclone Combustion Test Facility. Clean Coal Sustainable Energy 179–188. https://doi.org/10.1007/978-981-16-1657-0_14
39. Noh Y-H et al Ashless herbaceous biomass for slagging and fouling reduction in solid-fuel boiler: Combustion and ash fusion characterizations. Fuel 379:132957. https://doi.org/10.1016/j.fuel.2024.132957
40. Safar M et al Catalytic effects of potassium on biomass pyrolysis, combustion and torrefaction. Appl Energy 235:346–355. https://doi.org/10.1016/j.apenergy.2018.10.065
41. Quan S et al Ash thermomechanical properties and combustion characteristics during Co-combustion of anthracite and biomass for CFB combustors. Biomass Bioenergy 201:107868. https://doi.org/10.1016/j.biombioe.2025.107868
42. Han J, Yu D, Wu J, Yu X, Liu F, Xu M Effects of torrefaction on ash-related issues during biomass combustion and co-combustion with coal. Part 2: Ash fouling behavior. Fuel 334:126777. https://doi.org/10.1016/j.fuel.2022.126777
43. Zhu D, Yang H, Chen Y, Li Z, Wang X, Chen H Fouling and Slagging Characteristics during Co-combustion of Coal and Biomass. BioResources 12(3). https://doi.org/10.15376/biores.12.3.6322-6341
44. Chen X, Gao X, Wu H (2022) Characterization of Ashes from Co-Firing Biochar with Coal under Pulverized-Fuel Conditions, *ACS Engineering Au*, vol. 2, no. 5, pp. 397–405, Oct. https://doi.org/10.1021/acsengineeringau.2c00012
45. Niu Y, Tan H, Hui S Ash-related issues during biomass combustion: Alkali-induced slagging, silicate melt-induced slagging (ash fusion), agglomeration, corrosion, ash utilization, and related countermeasures. Prog Energy Combust Sci 52:1–61. https://doi.org/10.1016/j.pecs.2015.09.003
46. Li J, Long X, Zhu H, Liu Z, Lu X, Zhang D Investigation into the fusibility of biomass ashes and their mineral phase transformations at elevated temperatures by using the HT-XRD technique. Biomass Bioenergy 173:106812. https://doi.org/10.1016/j.biombioe.2023.106812
47. Bichang'a DO et al (2024) Comparative property investigation of raw and treated coconut shell biomass for potential polymer composite application, *Heliyon*, vol. 10, no. 23, p. e40704, Dec. https://doi.org/10.1016/j.heliyon.2024.e40704
48. Ashwini K, Resmi R, Reghu R Pyrolysis characteristics and kinetic analysis of coconut shell and nutmeg shell for potential source of bioenergy. Eng Sci Technol Int J 50:101615. https://doi.org/10.1016/j.jestch.2024.101615
49. Ansari KB et al Comprehensive review on biomass chemical looping combustion: Feedstock type, operating conditions, reactor design, technological advancement, mechanistic insights, and economics. J Environ Chem Eng 13(3):116947. https://doi.org/10.1016/j.jece.2025.116947
50. Zhou T, Chen X, Liu F, Miao F, Li C, Ding Y Pyrolysis behavior study of Cycas revoluta Thunb leaves and comparison based on its isolated components by Thermogravimetric/Fourier transform infrared analysis. Therm Sci Eng Progress 57:103099. https://doi.org/10.1016/j.tsep.2024.103099
51. Chen W-H, Kuo P-C (2010) A study on torrefaction of various biomass materials and its impact on lignocellulosic structure simulated by a thermogravimetry. *Energy,* 35(6):2580–2586. https://doi.org/10.1016/j.energy.2010.02.054
52. Deb Abhi T, Norouzi O, Macdermid-Watts K, Heidari M, Tasnim S, Dutta A Miscanthus to Biocarbon for Canadian Iron and Steel Industries: An Innovative Approach. Energies (Basel) 14(15):4493. https://doi.org/10.3390/en14154493
53. Singh S, Chakraborty JP, Mondal MK Optimization of process parameters for torrefaction of Acacia nilotica using response surface methodology and characteristics of torrefied biomass as upgraded fuel. Energy 186:115865. https://doi.org/10.1016/j.energy.2019.115865
54. Conag AT, Villahermosa JER, Cabatingan LK, Go AW (2017) Energy densification of sugarcane bagasse through torrefaction under minimized oxidative atmosphere. J Environ Chem Eng 5(6):5411–5419. https://doi.org/10.1016/j.jece.2017.10.032
55. Ohm T-I, Chae J-S, Kim J-K, Oh S-C (2015) Study on the characteristics of biomass for co-combustion in coal power plant. J Mater Cycles Waste Manag 17(2):249–257. https://doi.org/10.1007/s10163-014-0334-y